INTERNATIONAL JOURNAL OF CLIMATOLOGY
*Int. J. Climatol.* **19**: 835–861 (1999)

# LOCAL ESTIMATES OF GLOBAL CLIMATE CHANGE: A STATISTICAL DOWNSCALING APPROACH

SILVINA A. SOLMAN* and MARIO N. NUÑEZ

*Centro de Investigaciones del Mar y la Atmósfera (CIMA/UBA-CONICET), Departamento de Ciencias de la Atmósfera, Facultad de Ciencias Exactas y Naturales, Universidad de Buenos Aires, Buenos Aires, Argentina*

*Received 19 June 1998*
*Revised 30 November 1998*
*Accepted 30 November 1998*

## ABSTRACT

For the purposes of estimating local changes in surface climate at selected stations in the central Argentina region, induced by an enhanced $CO_2$ concentration, projected by general circulation models (GCM), a statistical method to derive local scale monthly mean minimum, maximum and mean temperatures from large-scale atmospheric predictors is presented. Empirical relationships are derived among selected variables from the NCEP re-analyses and local data for summer and winter months, tested against an independent set of observed data and subsequently applied to the HADAM and MPI GCM control runs. Finally, the statistical approach is applied to a climate change experiment performed with the MPI model to construct a local climate change scenario.

The comparison between the estimated versus the observed mean temperature fields shows good agreement and the temporal evolution of the estimated variables is well-captured, though, the estimated temperatures contain less interannual variability than the observations.

For the present day climate simulation, the results from the HADAM and MPI GCMs are used. It is shown that the pattern of estimated temperatures obtained using the MPI large-scale predictors matches the observations for summer months, though minimum and mean temperatures are slightly underestimated in the southeast part of the domain. However, the differences are well within the range of the observed variability.

The possible anthropogenic climate change at the local scale is assessed by applying the statistical method to the results of the perturbed run conducted with the MPI model. For summer and winter months, the local temperature increase is smaller for minimum temperature than for maximum temperature for almost all the stations, yielding an enhanced temperature amplitude in both seasons. The temperature amplitude (difference between maximum and minimum) for summer months was larger than for winter months. The estimated maximum temperature increase is found to be larger for summer months than for winter months for all the stations, while for the minimum, temperature increases for summer and winter months are similar. 

KEY WORDS: South America; Argentina; region; techniques; statistical downscaling; climate variables; regional climate change; monthly temperature

## 1. INTRODUCTION

The most promising method for predicting the future behaviour of the global climate system is the use of general circulation models (GCMs). These models have demonstrated their ability to simulate realistically the large-scale features of the observed climate (e.g. for the South American region, we can cite the more recent articles by Carril *et al.*, 1997 and Labraga, 1997), and hence, they are widely used to assess the impact that an increased loading of the atmosphere with greenhouse gases might have on the climate system. While there exists differences in modelling schemes, most models project comparable results on a global basis. However, they have difficulty in reproducing regional climate patterns, and large discrepan-

* Correspondence to: Centro de Investigaciones del Mar y la Atmósfera (CIMA/UBA-CONICET), Ciudad Universidad, Pabellón II, Piso 2, 1428 Buenos Aires, Argentina. Tel.: +54 119 7872693; fax: +54 119 7883572; e-mail: solman@at1.fcen.uba.ar

Contract/grant sponsor: European Commission; Contract/grant number: CEE C11-CT94-0111

CCC 0899–8418/99/080835–27$17.50

cies are found among models. In many regions of the world, the distributions of significant surface variables, such as temperature and rainfall, are often influenced by the local effects of topography and other thermal contrasts, and the coarse spatial resolution of the GCMs can not resolve these effects.

In recent years there has been increasing concern regarding the consequences of global climate change on natural and socio-economic systems due to enhanced greenhouse gases, especially $CO_2$. The assessment of climate change impacts on agriculture, hydrological and water resource systems often requires detailed and reliable climate change scenarios at regional and local scales, that cannot be resolved by current GCMs (Grotch and MacCracken, 1991). It has been recognized that the response of regional climate to global climate change is spatially heterogeneous due to local effects that cannot be taken into account with current GCMs and, consequently, large-scale GCM scenarios should not be used directly for impact studies (von Storch, 1994). Thus, in order to estimate the impact of climatic change on the local scale, an adequate means of relating GCM output to the local climate is required.

Different strategies have been developed to deduce local climatic estimates from global scale simulations; mainly the dynamical approach and statistical methods. All these strategies implicitly assume that the GCMs yield a reliable estimate on the large-scale. The dynamical approach involves the use of a nested limited area model (LAM) in a GCM over a considered region (Giorgi, 1990). The major advantage of this approach is that the regional simulations are dynamically consistent with the GCM large-scale results. However, this approach is computationally costly and feedbacks from the regional model into the GCM are not usually incorporated. Only very recently has the coupling of GCMs and LAMs begun to include two-way interaction (Déqué and Piedelievre, 1995; Leslie, 1995).

Another approach is to derive statistical relationships between observed local climatic variables and large-scale variables. Downscaling by statistical means has been increasingly developed over the last few years. All methods translate the large-scale GCM information into a high resolution distribution based on empirically derived relationships. A multiple regression technique was used by Wigley *et al.* (1990) to derive regression equations linking large-scale spatial averages of precipitation and surface temperature and other large-scale variables to local precipitation and temperature–time series on the west coast of the US. Many authors have demonstrated that air flow indices are useful predictors for regression-based downscaling to simulate local rainfall (Conway *et al.*, 1996; Kilsby *et al.*, 1998; Wilby *et al.*, 1998) and surface temperatures (Karl *et al.*, 1990; Winkler *et al.*, 1997). Hewitson (1994) constructed regression equations between the atmospheric circulation and local surface temperature, allowing a non-linear interaction among different atmospheric regimes. These methodologies make use of the GCM minimum scale (grid point) information to derive the statistical relationships. Other authors propose a mixed empirical–dynamic approach to translate the large-scale GCM information into a high resolution distribution, such as von Storch *et al.* (1993) who used canonical correlation analysis to develop relationships between large-scale monthly sea level pressure (SLP) fields and local monthly Iberian winter rainfall. They found that the method was skilful in reproducing the observed Iberian Peninsula precipitation anomalies from SLP fields. Schubert and Henderson-Sellers (1997) described a statistical method to derive information about local daily temperature extremes from larger atmospheric flow patterns in the Australian region. This methodology has also been used by other authors for model validation (e.g. Noguer, 1994; Burkhardt, 1995). All of these statistical methods make use of correlations between the time series of large-scale and local variables, though statistical techniques based on regression methods are suitable only for variables that are continuous in time and space, such as temperature. Other statistical approaches have been developed by many authors, such as non-parametric models (Corte-Real *et al.*, 1993), neural networks (McGinnins, 1994), WGEN methods (Katz and Parlange, 1996), stochastic weather generation algorithms (Wilks, 1992) and techniques based on weather classification schemes (Bardossy and Plate, 1992; Hughes *et al.*, 1993; Zorita *et al.*, 1995; Enke and Spekat, 1997) suitable for discontinuous variables, such as daily precipitation.

The advantages of the statistical approaches are that they are easy to implement, not computationally costly and calibration to the local level is an integral part of the procedure. It is also important to note that the results obtained using these methods have comparable accuracy with those obtained with dynamical downscaling techniques (see Jones *et al.*, 1997).

 

The reliability of the projected local changes will depend firstly, on the capability of the GCM in reproducing the large-scale variables that will be used to deduce the local climate. However, the results of any statistical method are conditioned by the implicit assumption that the relationship derived using historical records should explain a great part of the observed variability of the local variable, and will remain valid under changing conditions (von Storch *et al*., 1993).

The purpose of this work is to estimate local changes of monthly mean surface air temperature extremes for summer and winter months caused by $CO_2$ doubling, at selected stations lying in central Argentina, following the strategy first developed by Wigley *et al*. (1990). Despite the simplicity of the regression technique employed, the ability in determining local estimations from the large-scale variables selected is explored, by checking the assumptions cited above, in order to give some degree of confidence to the projected local temperature changes inferred from GCM outputs. Making use of the interannual variability of climate, empirical relationships are derived between selected variables from the National Center for Environmental Prediction (NCEP) re-analyses (Kalnay *et al*., 1996) and local minimum, maximum and mean air temperature at a monthly mean frame. These results are then tested against an independent set of observed data and subsequently applied to present day climate simulations conducted with GCMs. Finally, the statistical approach is applied to a climate change experiment performed with a GCM to construct a local climate change scenario.

The paper is structured in the following way. The data set used to derive the statistical relationships and the description of the method are presented in Section 2. The evaluation of the method and the results are described in Section 3. In Section 4 we first analyse the reliability of the Hadley Centre for Climate Prediction and Research GCM (HADAM) and the Max Plank Institut für Meteorologie Coupled GCM (MPI) in simulating the present day circulation. A complete description of the GCMs can be found in Cullen (1993) and Cubasch *et al*. (1992), respectively. Then the statistical scheme is applied to the control and $2 \times CO_2$ simulations to project the local estimates of climate change. Conclusions are presented in Section 5.

## 2. DATA AND STATISTICAL TECHNIQUE

The observational data used are monthly mean values of minimum, maximum and mean temperature at 31 selected stations covering the central region of Argentina during the period 1972–1994 for austral summer (December–January–February) and winter (June–July–August) months, provided by the National Weather Service of Argentina (SMN) and from the Instituto Nacional de Tecnología Agropecuaria (INTA). The stations are selected based on data quality and in order to assure an even cover over the region. Figure 1 and Table I provide information about the location, distribution and index of the stations and grid points used in this study.

Since the statistical relationships between large-scale and local scale variables should explain a great portion of the local scale temperature variability, the large-scale variables used to derive the statistical method should represent adequately the large-scale climate characteristics. In order to fulfil this condition, NCEP re-analyses of monthly mean data in a 2.5° grid covering the sector 65–55°W and 30–40°S for the same period are used. Figure 1 also shows the location and index of the grid points used. We will refer to these data as 'analyses'.

The condition noted above concerning the reliability of the large-scale variables should be pursued using the present day simulations of the GCMs, in order to give some degree of confidence in the global climate change estimates due to $CO_2$ doubling projected by the models, and hence, to the local estimates of global change. This topic will be addressed further on in this paper.

Following the methodology developed by Wigley *et al*. (1990), statistical relationships between large-scale climatic variables, the predictors, and local scale minimum, maximum and mean temperature, the predictands are derived by means of the multiple regression technique. We make use of interannual variability in climate to derive the empirical relationships. The data used are divided into a calibration set and an independent verification set. The equations are calibrated using the 1982–1994 period and an

 

independent verification period for years 1972–1981 is used to test the results against the known observed variables.

It is desirable that the calibration period be as long as possible to increase the reliability of the statistical analysis and to allow a range of natural variability, assuming that the expected changes in the mean climate would lie within the range of natural variability (von Storch *et al*., 1993). In this study, the calibration period comprises 13 years of data. With the aim of overcoming the first requirement cited above, concerning the length of the calibration period, instead of using the time series of monthly mean data, summer and winter month samples are constructed, so that for each season the data sample consists of 39 months. The second requirement, concerning the range of variability, is analysed further on, in terms of the analysis of the standard deviation of the predictands versus the range of variability of the climatic change projected by the GCMs.

According to von Storch *et al*. (1993), the large-scale variables selected as predictors have to be strongly linked to the local predictands. In this context, the predictor variables from the NCEP re-analyses selected to derive the equations for minimum, maximum and mean station temperature, are: air temperature at 2 m, mean sea level pressure and zonal and meridional components of the wind at 200 and 700 hPa. With the exception of the large-scale temperature at 2 m, which has an obvious relationship with local temperatures, the other predictor variables add information about the circulation conditions. The zonal and meridional components of the wind at 700 hPa take into account the advective effect; the mean sea level pressure captures information about large-scale circulation; and 200 hPa, winds add information about the position of the subtropical jet, which influences the characteristics of the tropospheric

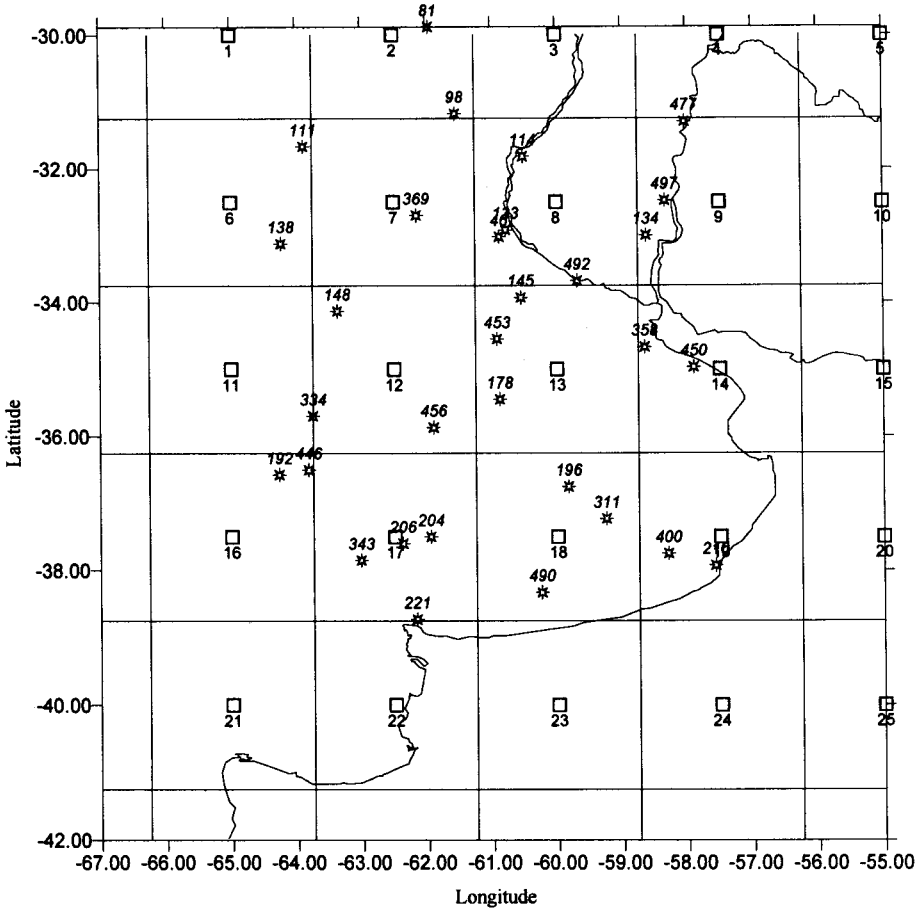


Figure 1. Location and index of stations (asteriks) and grid-points (squares) used in this study

 

Table I. Names, location and index of stations and grid points used in the analysis

| Station name | Longitude (°W) | Latitude (°S) | Station number |
|---|---|---|---|
| Rafaela | 61.55 | 31.18 | 98 |
| Pilar | 63.88 | 31.67 | 111 |
| Rosario | 60.78 | 32.92 | 133 |
| Rio Cuarto | 64.23 | 33.12 | 138 |
| Pergamino | 60.55 | 33.93 | 145 |
| Laboulaye | 63.37 | 34.13 | 148 |
| 9 de Julio | 60.88 | 35.45 | 178 |
| Sta. Rosa | 64.27 | 36.57 | 192 |
| Azul | 59.83 | 36.75 | 196 |
| Pigüé | 62.38 | 37.60 | 206 |
| Mar del Plata | 57.58 | 37.93 | 210 |
| Bahia Blanca | 62.17 | 38.73 | 221 |
| Gral. Pico | 63.75 | 35.70 | 334 |
| Castelar | 58.65 | 34.67 | 358 |
| Marcos Juarez | 62.15 | 32.70 | 369 |
| La Plata | 57.90 | 34.97 | 450 |
| Pehuajó | 61.90 | 35.87 | 456 |
| Tres Arroyos | 60.25 | 38.33 | 490 |
| San Pedro | 59.68 | 33.68 | 492 |
| Anguil | 63.82 | 36.50 | 446 |
| Balcarce | 58.30 | 37.75 | 400 |
| Bordenave | 63.02 | 37.85 | 343 |
| Ceres | 61.95 | 29.88 | 081 |
| Concep. del Uruguay | 58.33 | 32.48 | 497 |
| Concordia | 58.02 | 31.30 | 477 |
| Coronel Suarez | 61.95 | 37.50 | 204 |
| Gualeguaychú | 58.62 | 33.00 | 134 |
| Paraná | 60.51 | 31.82 | 114 |
| Tandil | 59.25 | 37.23 | 311 |
| Zavalla | 60.88 | 33.02 | 046 |
| Junin | 60.92 | 34.55 | 453 |

circulation. These variables have been used by other authors, such as Karl *et al.* (1990) and Wigley *et al.* (1990), who included mean sea level pressure and 850 and 500 hPa winds as predictors. These predictor variables are found to be highly correlated with the predictands, as can be seen in Table II, which shows

Table II. Spatial average of significant ($p > 0.95$) correlation coefficients ($r$) between predictors and predictands (station minimum, maximum and mean temperatures)

| Predictors | Summer months | | | | | | Winter months | | | | | |
|---|---|---|---|---|---|---|---|---|---|---|---|---|
| | Minimum | | Maximum | | Mean | | Minimum | | Maximum | | Mean | |
| | *r* | *n* | *r* | *n* | *r* | *n* | *r* | *n* | *r* | *n* | *r* | *n* |
| TG | 0.64 | 31 | 0.82 | 31 | 0.81 | 31 | 0.81 | 31 | 0.80 | 31 | 0.93 | 31 |
| PG | −0.48 | 24 | −0.40 | 9 | −0.44 | 22 | −0.56 | 30 | −0.39 | 18 | −0.47 | 16 |
| UG2 | −0.41 | 7 | −0.40 | 12 | −0.40 | 11 | −0.36 | 15 | −0.35 | 5 | −0.35 | 10 |
| VG2 | −0.38 | 21 | −0.36 | 10 | −0.41 | 12 | — | | — | | — | |
| UG7 | −0.41 | 28 | −0.44 | 15 | −0.42 | 21 | — | | — | | — | |
| VG7 | −0.41 | 16 | −0.42 | 9 | −0.44 | 9 | −0.40 | 20 | −0.39 | 13 | −0.38 | 16 |

*n* indicates the number of stations in which the correlation is significative.
Abbreviations: TG, temperature at 2 m; PG, sea level pressure; UG2, 200 hPa zonal wind; VG2, 200 hPa meridional wind; UG7, 700 hPa zonal wind; VG7, 700 hPa meridional wind.

 

Table III. Spatial average of the percentage of explained variance for the calibration period (1982–1994) using 2 m large-scale temperature as the only predictor variable and using all predictors and in verification period, 1972–1981 (using all predictors)

| $\sigma$ (%) (S.E.) | Summer months | | | Winter months | | |
|---|---|---|---|---|---|---|
| | Calibration | | Verification | Calibration | | Verification |
| | TG | All predictors | All predictors | TG | All predictors | All predictors |
| Minimum | 49.3 | 75.9 (0.47) | 56.4 (0.80) | 66.6 | 77.5 (0.81) | 61.6 (1.25) |
| Maximum | 67.1 | 75.8 (0.68) | 58.9 (1.20) | 65.2 | 73.5 (1.03) | 53.2 (1.20) |
| Mean | 68.5 | 82.5 (0.35) | 61.9 (0.95) | 86.1 | 89.3 (0.28) | 77.4 (0.52) |

Standard errors (S.E.) are given in parenthesis.

the correlation coefficients between the predictor and predictand variables. Another condition taken into account in the selection of the predictor variables is that the large-scale variables acting as predictors in the statistical model had to be well-simulated by the GCMs. If the GCM fails in reproducing reasonably well the present large-scale climate characteristics, any downscaling procedure will fail. This condition is reasonably satisfied by the list of predictors used (see Carril *et al.*, 1997).

A separate equation is derived for each station by regressing the reference set of observed temperatures (minimum, maximum and mean) versus the large-scale variables, considering for each grid box the stations which lie within it. For each station $i$, only the nearest grid point, $n$, is considered (see Figure 1 for reference). The equations are then of the form:

$$T'_{i,m} = a_{i,m} + b_{i,m}\mathrm{TG}_{n,m} + c_{i,m}\mathrm{PG}_{n,m} + d_{i,m}\mathrm{UG2}_{n,m} + e_{i,m}\mathrm{VG2}_{n,m} + f_{i,m}\mathrm{UG7}_{n,m} + g_{i,m}\mathrm{VG7}_{n,m} + e$$

where the subscript $m$ indicates the season and $T'_{i,m}$ is the temperature estimated at station $i$; $\mathrm{TG}_{n,m}$ is the temperature at grid point $n$; $\mathrm{PG}_{n,m}$ is the mean sea level pressure at grid point $n$; $\mathrm{UG2}_{n,m}$ is the 200 hPa zonal component of the wind at grid point $n$; $\mathrm{VG2}_{n,m}$ is the 200 hPa meridional component of the wind at grid point $n$; $\mathrm{UG7}_{n,m}$ is the 700 hPa zonal component of the wind at grid point $n$; $\mathrm{VG7}_{n,m}$ is the 700 hPa meridional component of the wind at grid point $n$; $a_{i,m}$, $b_{i,m}$, $c_{i,m}$, $d_{i,m}$, $e_{i,m}$, $f_{i,m}$ and $g_{i,m}$ are the regression coefficients for each station $i$; $e$ is the residual error term.

The regression equations are derived using stepwise multiple regression, in which each predictor variable is evaluated for its individual significance level before being included in the equation and, with each addition, each variable within the equation is then evaluated for its significance as part of the model. A variable is included in the equation if it is significant at the 95% level and is retained if it is significant at the 99% confidence level.

For all the stations, in summer and winter months, large-scale temperature is the predictor that explains most of the predictand variance (as expected), while the other variables contribute an additional percentage that varies with the predictand variable, station and time of the year. Results for minimum, maximum and mean temperature for summer and winter months are summarized on Table III. Table IV lists, by site, the predictor variables retained by the stepwise linear regression for each predictand, for summer and winter months, respectively.

For almost all the stations, large-scale temperature, mean sea level pressure and 700 hPa zonal wind are the predictor variables retained in the regressive models, while the other predictor variables contribute significantly only for some locations.

As mentioned before, the statistical method developed is based on statistical relationships between large-scale climatic variables and local scale temperatures, making use of the interannual variability of climate. Moreover, one of the assumptions underlying the applicability of the statistical technique to climate change scenarios is that the projected changes of the mean climate should lie within the natural variability of the observed climate. In other words, we must assume that expected altered mean climate is sufficiently near the present one. In this context, it is pertinent to examine the mean interannual

 

Table IV. List of predictor variables retained by the stepwise linear regression for each predictand, at each station used in the analysis

| Site | Minimum | Maximum | Mean |
|---|---|---|---|
| Summer months | | | |
| 98 | T,U2,V2,U7 | T,U2 | T,U2,V2 |
| 111 | T,P,U2,V7 | T,U2 | T,U2,P,V2,V7 |
| 133 | T,P,U7 | T,U7 | T,U7,V2,P |
| 138 | T,V2,U7,P | T,U2 | T,V2,U2 |
| 145 | T,V2,U7,P,U2 | T,P,U7 | T,U7,P |
| 148 | T,U7,V2,P,V7 | T,U2,V7 | T,P,U2,V2,V7 |
| 178 | T,V2,U7,P,U2 | T,U7 | T,U7,P |
| 192 | T,U7,V2,P,V7 | T,V2 | T,P,U2,V7 |
| 196 | T,V2,U7,P,V7 | T,U7 | T,P,U7 |
| 206 | T,V2,U7,P,V7 | T,U2,P,V2 | T,P,U7 |
| 210 | T,P,U7,V7 | T,U7,V7 | T,P,U7 |
| 221 | T,P,U7,V7 | T,V2,P,U7 | T,P,U2 |
| 334 | T,V2,U7 | T,V2,U7 | T,U7,V7 |
| 358 | T,P,U7,V7 | T,P | T,P,U7,V2 |
| 369 | T,P,U7,V2,U2 | T,U2,V7 | T,U2,P,U7 |
| 450 | T,V7,P,U7 | T | T,P,U7 |
| 456 | T,V2,U7 | T,U7,V7 | T,U7 |
| 490 | T,V2,U7,P | T,V2,U7,P | T,P,U7 |
| 492 | T,P,U7,V2,U7 | T,V2,U7,P | T,U7,V2,P |
| 446 | T,V2 | T,U2,V2,U7,V7 | T,V7 |
| 400 | T,V2,P,U7,V7 | T,V2,V7 | T,V7,P,V2 |
| 343 | T,U7,P,V2,V7 | T,V2,P,U2 | T,P,U2,U7 |
| 081 | T,V2,U2,V7 | T,U2,P | T,U2,V2,V7 |
| 497 | T,V7,P,U7 | T,U7 | T,U7,V7,V2 |
| 477 | T,V7,P,U7 | T,U2,V7 | T,P,U2,U7 |
| 204 | T,V2,U7,P | T,U2,P | T,U2,V7 |
| 134 | T,V7,P,U7 | T,U7 | T,U7,V2,P |
| 114 | T,V2,U7,P | T,U2 | T,U7,V2 |
| 311 | T,V2,U7,P | T,U7,V7 | T,U7,P |
| 046 | T,P,U7 | T,U7,V2 | T,P,U7 |
| 453 | T,V2,U7,U2 | T,V7 | T,V2,P,U7 |
| Winter months | | | |
| 98 | T | T,P | T,V7 |
| 111 | T,U2,P | T,U7,U2,V7 | T,U7,P,V7 |
| 133 | T,P,U2,V7 | T,U7 | T,P,U2 |
| 138 | T,P,U2 | T,V2,U2 | T,U7,P,V7 |
| 145 | T,P,U2 | T,V2 | T,P |
| 148 | T,P,U2 | T,P | T,U2 |
| 178 | T,P | T,V2,P | T,V7 |
| 192 | T,P | T,P | T,U7 |
| 196 | T,P,U7,U2 | T,P,U2 | T,U2,V7 |
| 206 | T,P | T,P,U2,V7 | T,P |
| 210 | T,P,V7 | T,P,V7 | T |
| 221 | T,V7 | T,P | T,P,U2 |
| 334 | T,P,U2 | T,P | T,V7 |
| 358 | T,P,V7 | T,P | T |
| 369 | T,P,U2 | T,U2 | T,P,U2,V7 |
| 450 | T,P,V7,U2 | T,P | T |
| 456 | T,P | T,P | T,V7 |
| 490 | T,P | T,P | T,U7 |
| 492 | T,P,U2,V7 | T | T,P,U2,V7 |
| 446 | T,P,U2 | T,P | T,V7 |
| 400 | T,U7,P,V7 | T,P,V2 | T,P |

 

Table IV. (continued)

| Site | Minimum | Maximum | Mean |
|---|---|---|---|
| 343 | T,V2 | T,P,U2 | T,P,U2 |
| 081 | T,P | T,V7 | T,P,U7 |
| 497 | T,P,U2,V7 | T,U2 | T,P,U2,V7 |
| 477 | T,P,U2,V7 | T,U2 | T,U2,P,V7 |
| 204 | T,P | T,P,U2 | T,U7,U2 |
| 134 | T,P,V7 | T,U2 | T,U2,P,V7 |
| 114 | T,P,U2 | T,V2 | T,P,V2,V7 |
| 311 | T,P | T,P,U2 | T,V7 |
| 046 | T,P,U2 | T,V2 | T,P |
| 453 | T,P,V7 | T,V2,P | T |

variability of the predictands and of the main predictor variable, the large-scale 2 m temperature, ($TG_{n,m}$), during the training period, in order to check consistency between both patterns.

Figure 2 shows the mean interannual standard deviations of the observed minimum, maximum and mean temperature and of the temperature at 2 m from the analyses for summer and winter months. The observed temperatures show a variability maximum over the northern part of the domain and minimum values at the coastal regions, reflecting the moderating influence of the ocean. The large-scale temperature replicates quite well the variability distribution, though it tends to be less variable than the observations, due to the fact that the grid point represents the spatial average within the grid box.

The consequence of this, as it will be shown in next section, is that the estimated temperature samples will represent lower variability when compared with observations.

## 3. RESULTS OF THE REGRESSION

The validity of the statistical method developed will be tested in terms of the spatial distribution of the percentage of observed variance explained by the regression and the comparison between the estimated versus the observed mean temperature fields for the independent verification period. We also analysed the spatial autocorrelation patterns of the observed and the estimated temperature fields, to check spatial consistency of the downscaled variables. In order to evaluate how well the statistical model captures the interannual variability of the predicted variables, the model has been tested using simulations of the interannual variability of mean, minimum and maximum temperatures. Results for selected stations are shown.

Figures 3 and 4 display the percentage of observed variance explained by the statistical method for minimum, maximum and mean temperature for summer and winter months, for the calibration and independent verification periods, respectively. The overall results are summarized in Table III, which displays the explained variances and standard errors of estimation averaged over all sites, for the calibration and verification periods, respectively.

For most of the stations, a substantial part of the observed variability can be explained by the large-scale predictor variables, though the performance of the model varies from site to site. In general, the model performs better in the south-eastern part of the domain. This can be due to the fact that the stations in this area are mostly under the influence of large-scale activity associated with the extratropical westerlies and also due to smaller interannual variability, as was previously noted. Except for maximum temperature, predictability is slightly better for winter months, probably due to large-scale synoptic systems, which control the dominant processes during this period of the year, while for summer months smaller scale processes, not well-captured by the large-scale predictors, are also important.

The performance of the regression model is similar for minimum and maximum temperatures, but is noticeably better for mean temperature. This can be attributed to the fact that the main large-scale

 

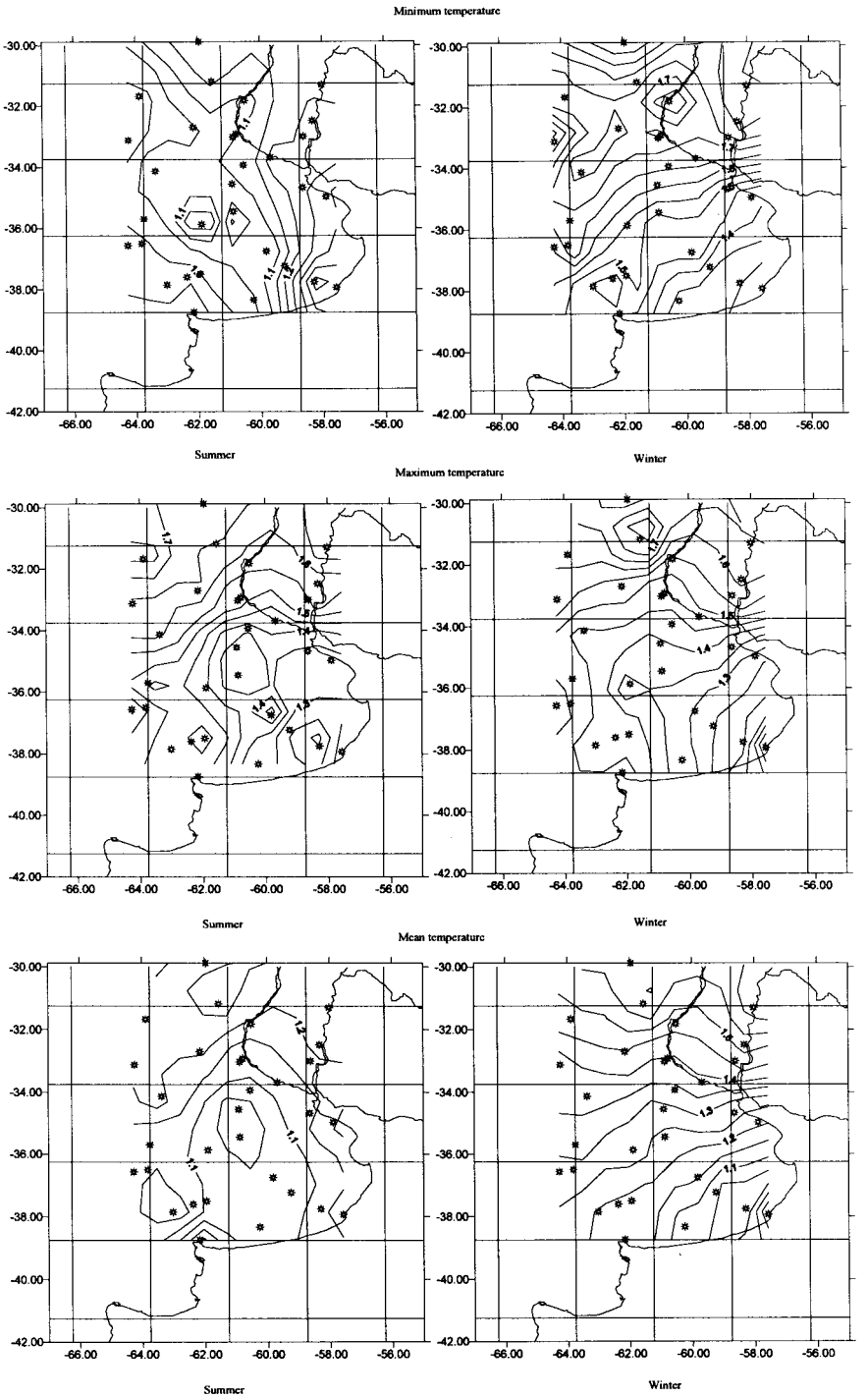


Figure 2. Standard deviation (°C) of minimum, maximum and mean temperatures as derived from observed data and standard deviation of 2 m temperature from NCEP re-analyses for the calibration period for summer months (left panels) and winter months (right panels)

 

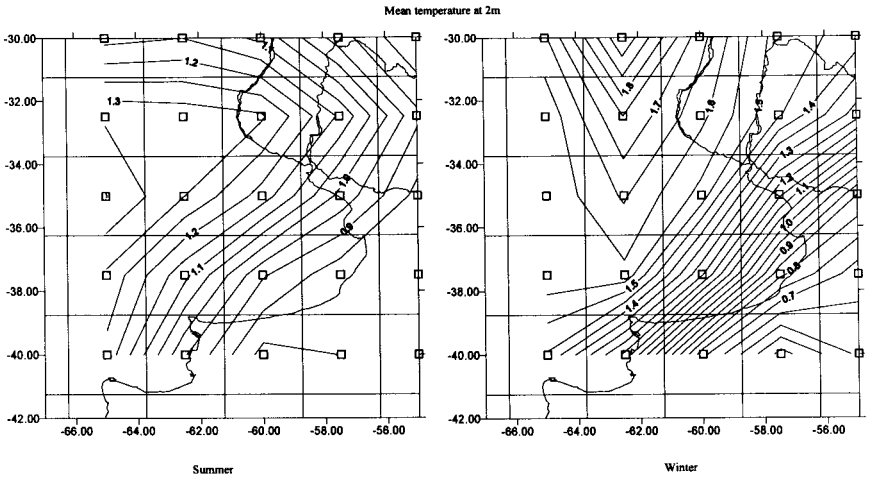


Figure 2 (*Continued*)

predictor is the mean temperature at 2 m. Large-scale temperature extremes or other variables that take into account the content of water vapour in the atmosphere, relevant for the minimum and maximum temperatures, are not used as predictors since they are not as well simulated by GCMs as mean temperature.

The area averaged explained variances, shown in Table III, are comparable with those obtained by other authors using different methodologies (e.g. in Wigley *et al.*, 1990; Burger, 1996; Schubert and Henderson-Sellers, 1997; Wilby *et al.*, 1998).

The explained variance declines on average by 20% between calibration and independent verification. This result is similar to that obtained in other studies (Wigley *et al.*, 1990).

Another test of the model performance is conducted by comparing the estimated field of the predictands versus the observed temperatures, averaged over the verification period. Figures 5 and 6 show the minimum, maximum and mean temperatures, estimated and observed for summer and winter months, respectively.

The spatial pattern of estimated minimum, maximum and mean temperatures match well with observations. Note also that the horizontal gradients are in good agreement. Maximum temperature is slightly underestimated for summer months over the whole domain, with an error of less than 1°C, less than the range of the natural variability shown in Figure 2. This can be due to the strong influence of convective processes during this season, not well-captured by the large-scale predictors, as mentioned before.

The patterns of spatial autocorrelation for the estimated temperature fields are compared with observations and with the main large-scale predictor, temperature at 2 m. Results for maximum temperature for summer months are shown in Figure 7. We can confirm from Figure 7 that the estimated temperature field is consistent with the observations in terms of the spatial autocorrelation.

Significance testing of station means and variances has also been done to test the performance of the statistical model in its different phases (calibration and verification). We used the standard $t$-test for evaluating differences in the means and Levene's test for differences in the standard deviations. The null hypothesis is rejected at a significance level of 5% for the means and at 10% for the standard deviations. Results for both, calibration and independent verification periods showed that for all locations, the estimated series of minimum, maximum and mean temperatures do not differ significantly from the observed series.

For climate impact studies, however, not only must the time-averaged spatial distribution of the temperature be properly estimated, but the interannual variability is also important. Hence, the model has been tested regarding its performance in capturing the time evolution and the interannual variability of

 

predictands. Many studies have carried out the evaluation of the statistical model in terms of the analysis of the estimated versus observed time series for area-averaged predictands (Corte-Real *et al.*, 1993; von Storch *et al.*, 1993; Noguer, 1994). Nevertheless, the evaluation of the temporal evolution of the spatial

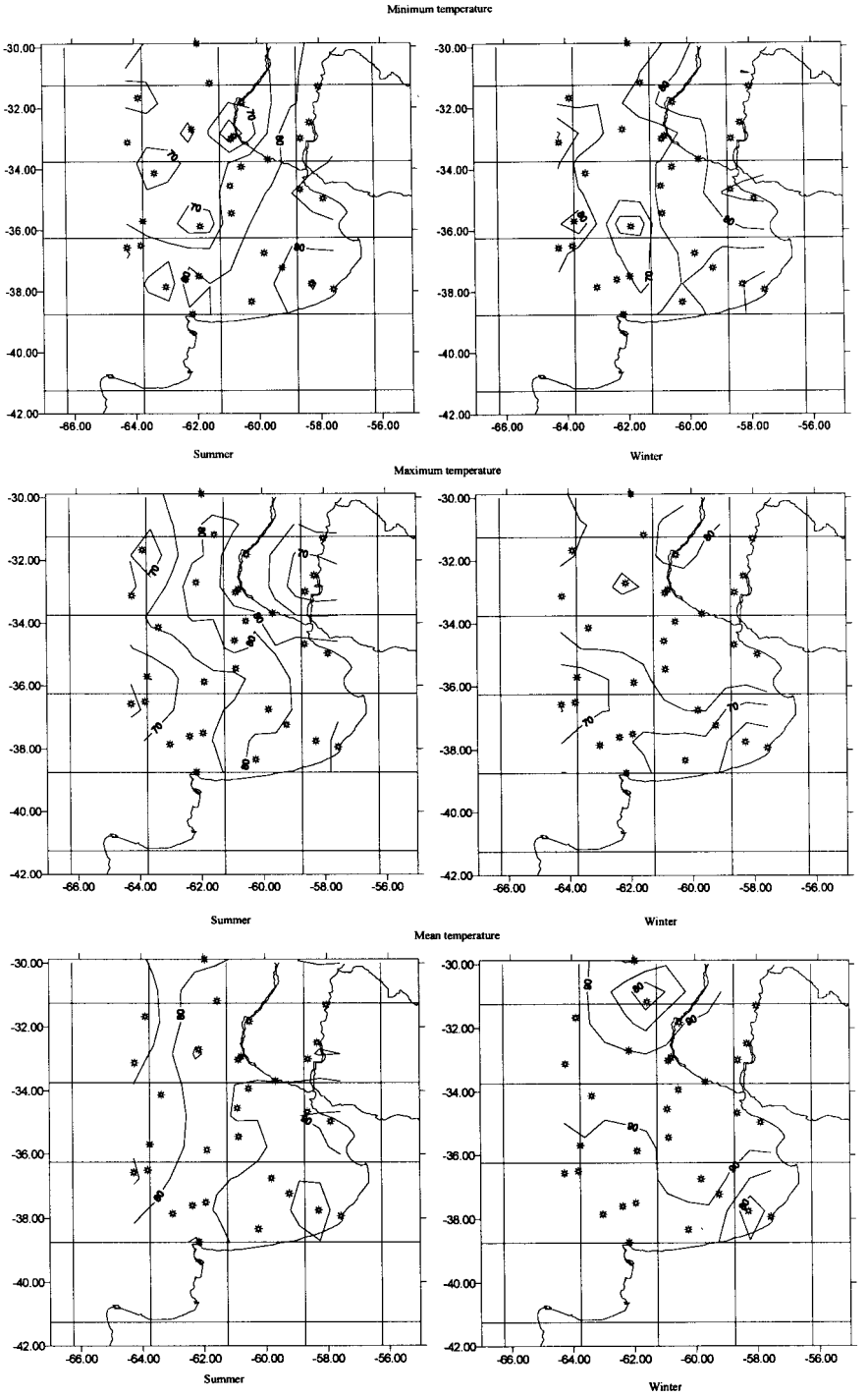


Figure 3. Spatial pattern of explained variance in calibration for summer (left panel) and winter months (right panel) for the minimum (top), maximum (centre) and mean (bottom) temperatures

 

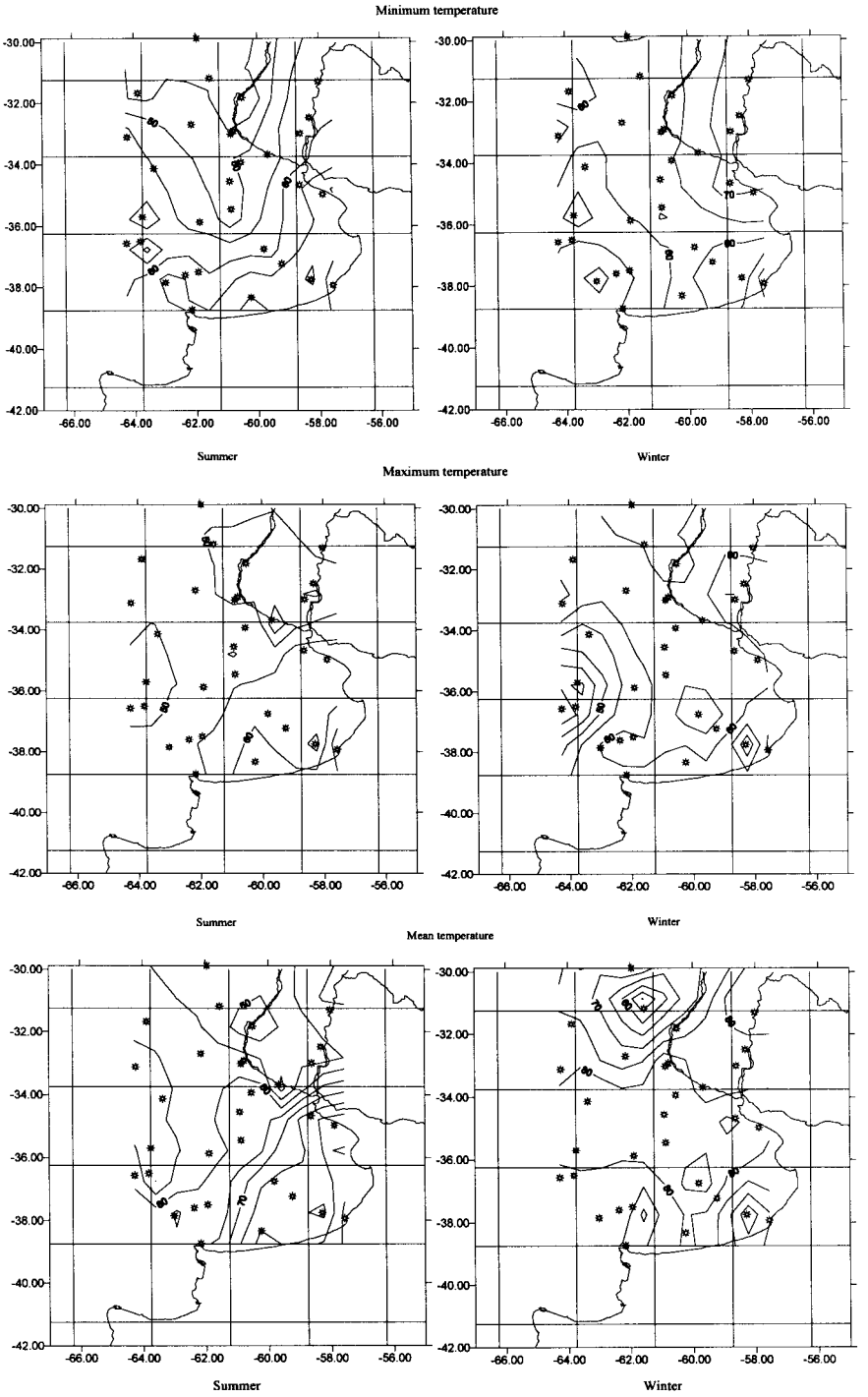


Figure 4. Same as Figure 3 for the verification period

average would obscure the model's ability in capturing the local scale variability, particularly if the stations are distributed in an a region of marked topographic or land–ocean contrasts. In this study, the temporal evolution of the resulting statistical prediction of minimum, maximum and mean temperatures at selected stations is compared against the observations for the verification period (1972–1981). Note

 

that we are not working strictly with time series, instead, each year number on the time axis in the graphs represents December, January and February (DJF) of year 1972 (June, July and August for winter) (JJA) of year 1973, and so on, until year 1981.

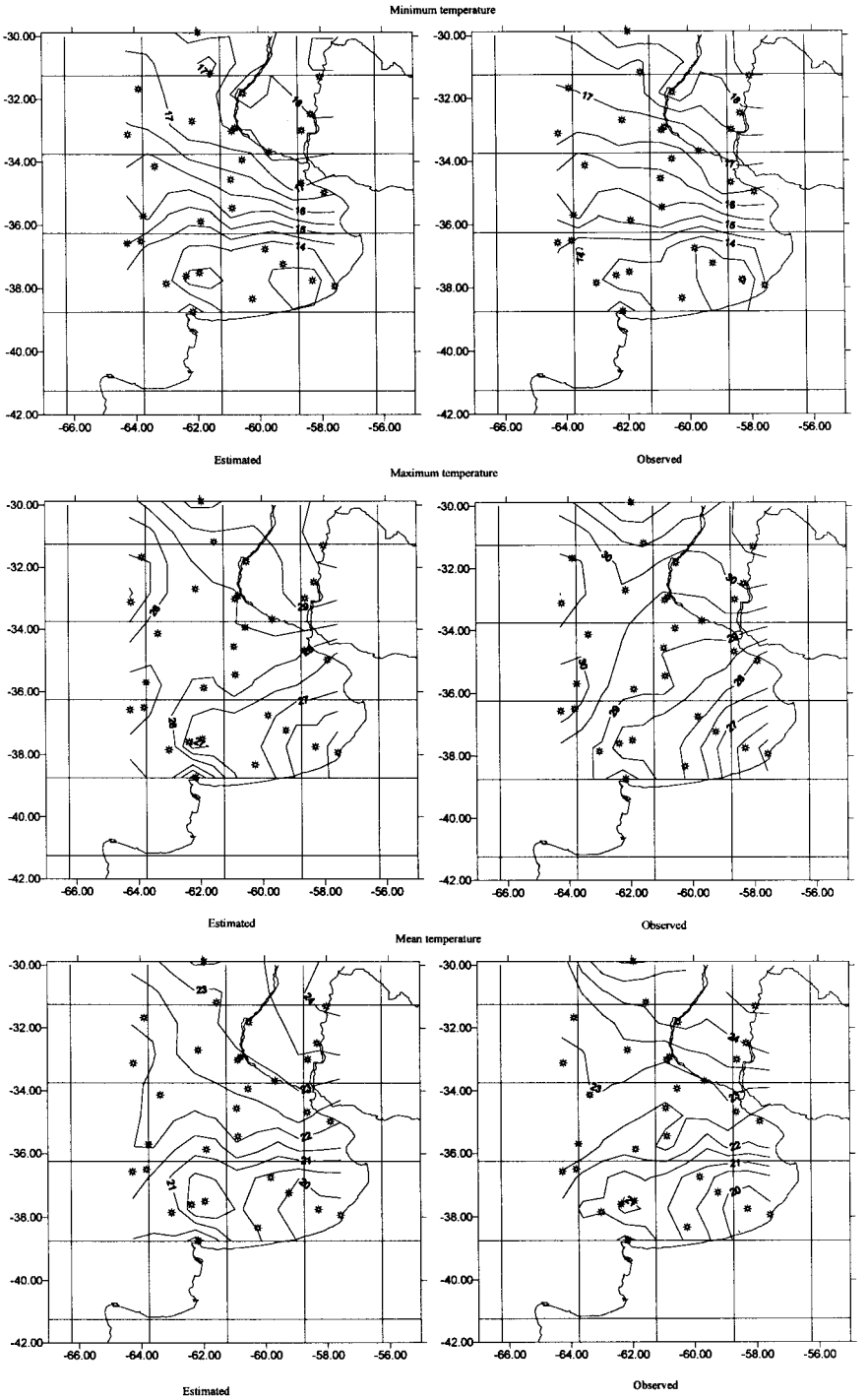


Figure 5. Mean fields of estimated (left panels) and observed (right panels) minimum (top), maximum (centre) and mean (bottom) temperatures averaged over the verification period for summer months

 

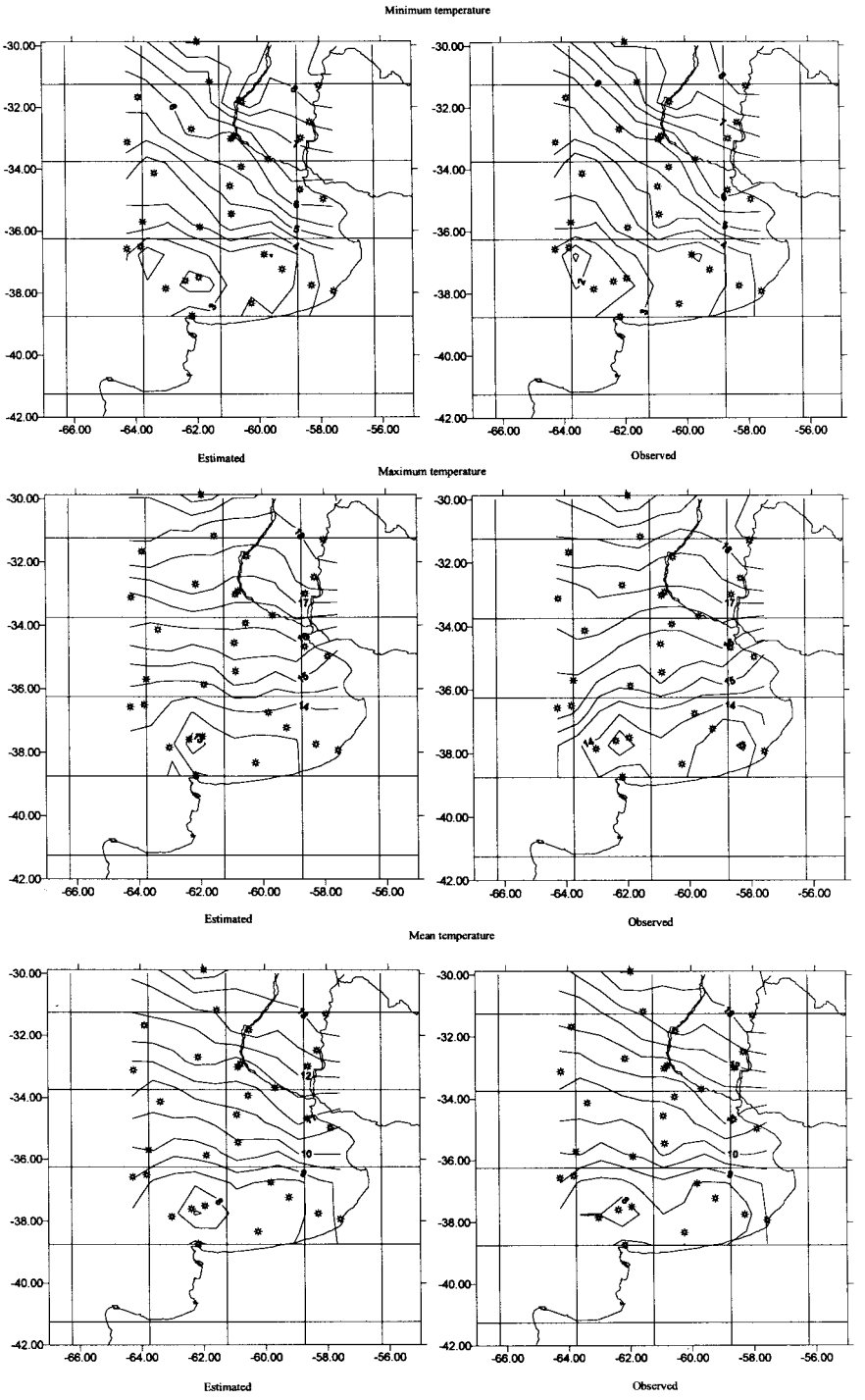


Figure 6. Same as Figure 5 for winter months

The results for four of the stations, Castelar (358), Azul (196), Mar del Plata (210) and Pergamino (145) are shown in Figure 8, where the estimated versus observed minimum, maximum and mean temperatures for summer and winter months are shown. The selection of these stations was made on the basis of their geographical locations. Mar del Plata is on the southern coast, strongly influenced by the land–sea

 

contrast, Castelar and Pergamino are influenced by thermal contrasts due to the presence of wide rivers and Azul is in a region without any significant thermal contrast. It can be seen that the regression equations capture the temporal evolution quite well, though as previously noted, the estimated tempera-

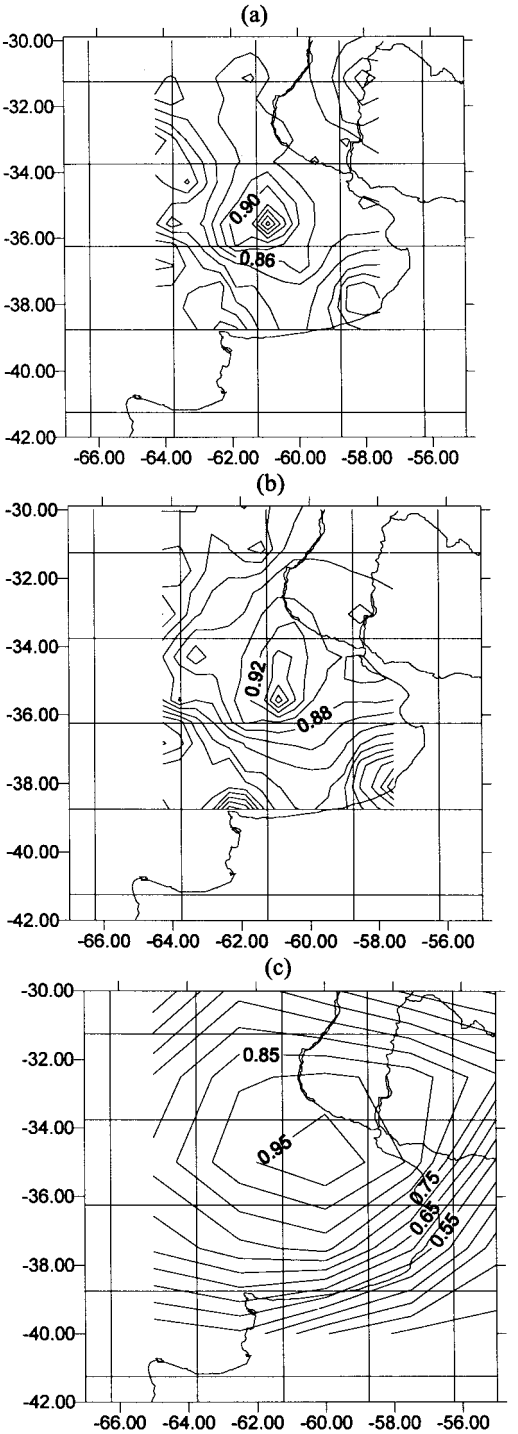


Figure 7. Patterns of spatial autocorrelation of observed (a) and estimated (b) maximum temperature and temperature at 2 m from the NCEP re-analysis (c) for summer months

 

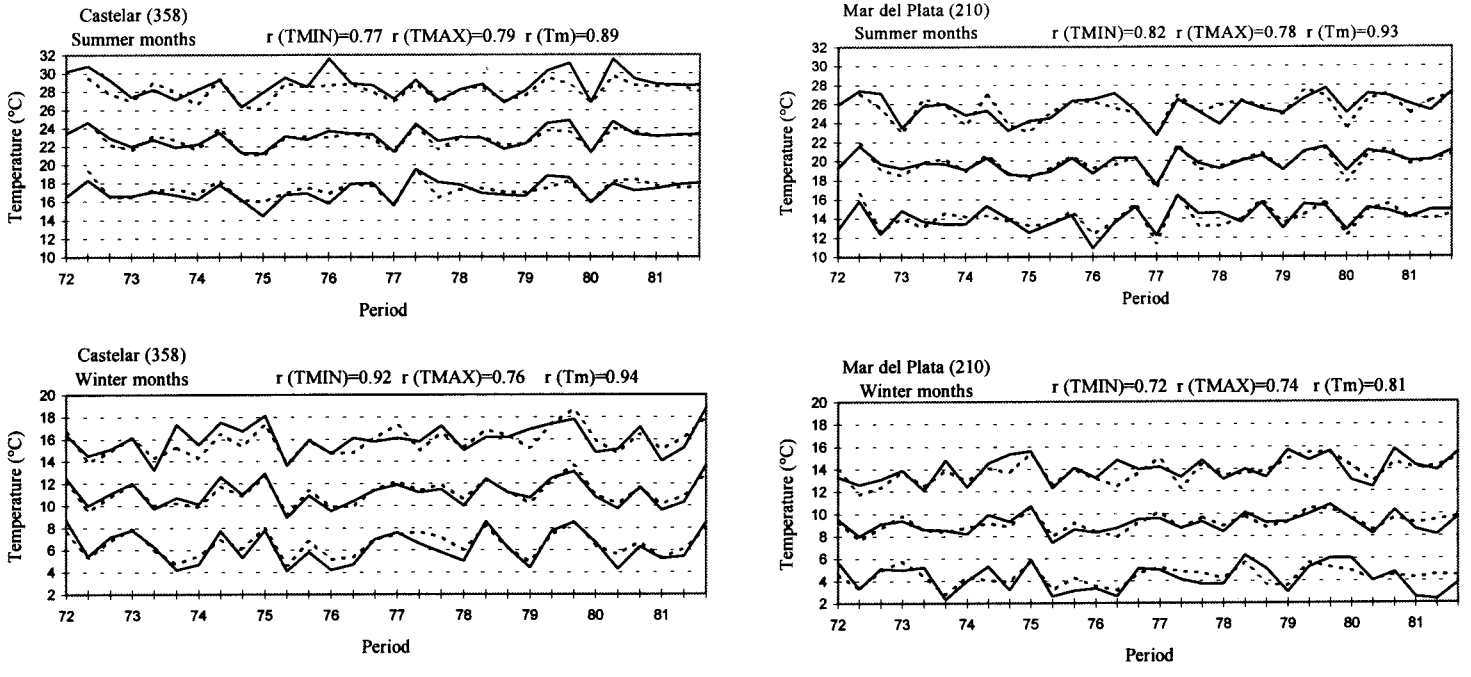


Figure 8. Statistical estimations (dashed lines) of minimum, maximum and mean temperatures at stations Castelar (358), Mar del Plata (210), Pergamino (145) and Azul (196) compared against observations (solid lines) for the verification period for summer and winter months. The correlation coefficient ($r$) between the estimated and the observed series is given

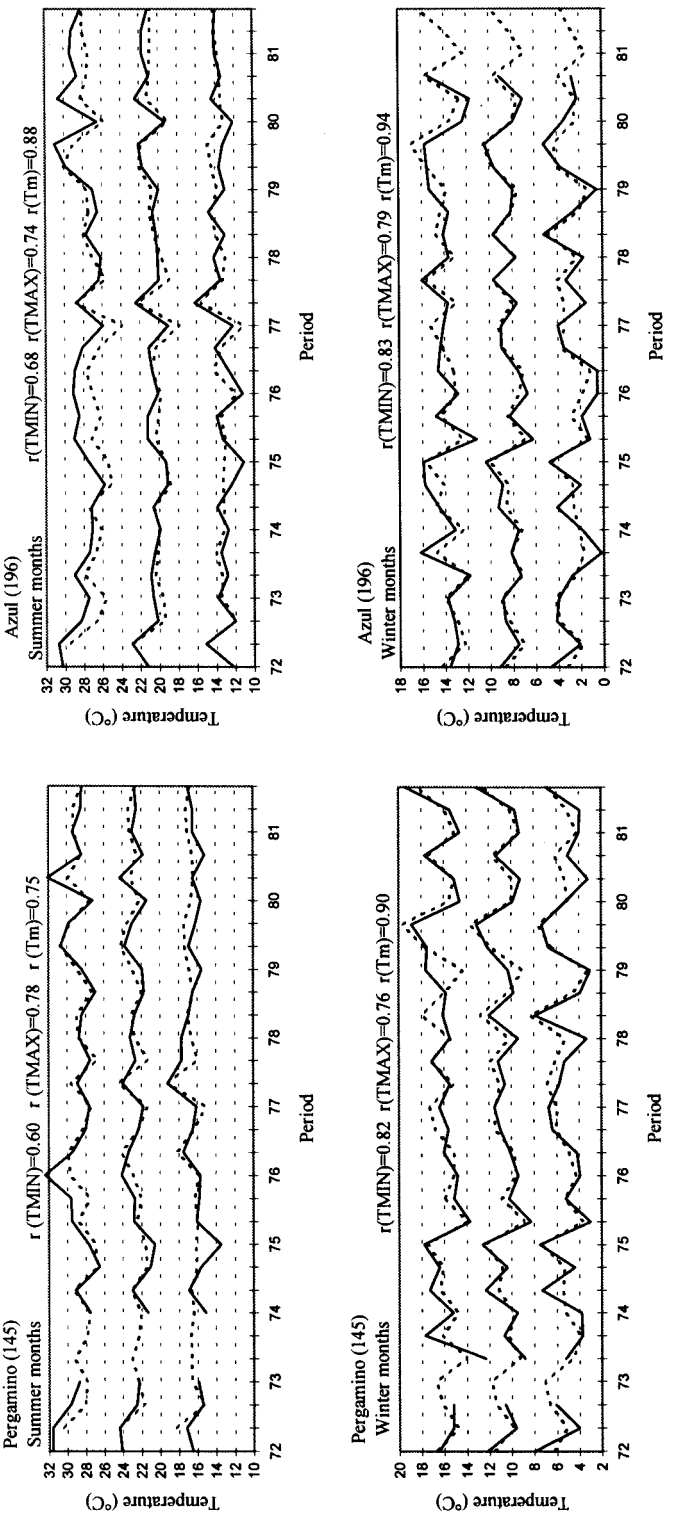


Figure 8 (*Continued*)

tures contain less interannual variability than the observed temperatures. The statistical model also captures the weaker interanual variability observed for summer months compared with winter months. It is also important to note that positive/negative anomalies of the observed samples (not shown) are represented by positive/negative anomalies of the estimated samples. It appears that for some locations, the estimated versus observed curves show a slight underestimation of the maximum temperature for summer months and better agreement is found for the mean and minimum temperatures. This may be an artefact of the predictor variables selected to calibrate the equations. Maximum temperatures are not as well-estimated as minimum temperatures, probably due to the fact that the maximum temperature is more strongly controlled by other factors, such as soil moisture and cloudiness, which have not been taken into account. However, the evolution of the estimated and observed variables are highly coherent and the general performance of the statistical model is quite reasonable, bearing in mind the simplicity of the model and the limitations due to the size of the data set used to fit the model. Once a good performance of the statistical model has been demonstrated using an independent verification period, we could re-calculate the regression coefficients using the whole data sample, the period 1972–1994, with the aim of improving their statistical reliability.

The successful reconstruction of the summer and winter monthly mean temperatures from the large-scale predictors indicates that the procedure developed may be used with GCM data, on the condition that the credibility of GCM simulated large-scale predictor variables used is satisfied. Assuming that the relationships derived will be maintained in a global change scenario, it is possible to project the global change at the local scale.

## 4. APPLICATION OF THE STATISTICAL METHOD TO GCM OUTPUTS

In this section, the statistical model developed and tested against observations will be applied to GCM simulated large-scale variables.

Results from three climate simulations are used in this study. For the present day climate simulation, the results from HADAM and MPI GCMs are used. HADAM is the first version of the Hadley Centre Atmospheric Model, with prescribed sea surface temperatures. It is a grid point model with a horizontal resolution of 2.5° latitude by 3.75° longitude and 19 hybrid levels in the vertical. The reference climate is obtained by a 49 year control integration with a fixed concentration of $CO_2$ of 321 ppmv, which is equivalent to the observed $CO_2$ concentration of the early 1950s. A detailed analysis of the performance of the model can be found in Murphy (1995). The data available for use are monthly means of 2 m air temperature, mean sea level pressure and zonal and meridional components of the wind at 200 and 700 hPa. Since there are missing values in the first years of the integration, only 45 years of data, from January 1948 to December 1992 are employed in this study. A constant concentration of $CO_2$ is used throughout the 45 year control simulation. This experiment assumes that the $CO_2$ in the control simulation is in a quasi-equilibrium state, though the real climate is in a transient state. Consequently, it is inappropriate to assign a model year to a calendar year, so that the climatology of the control simulation will be used as the present climate in this work.

The atmospheric component of the MPI climate model is the ECHAM-2 model, with a horizontal resolution of $5.6° \times 5.6°$ and 19 vertical levels. A complete description of this model can be found in Cubasch *et al.* (1992). The MPI ocean model includes cross-isopycnal mixing, convective exchange and a mixed-layer model. The deep ocean uses eight isopycnal levels in the vertical.

Possible anthropogenic climate change at local scale will be assessed by applying the statistical method to the results of the perturbed run conducted with the MPI coupled ocean–atmosphere model. For the perturbed simulation, the IPCC 'A' scenario is assumed (IPCC, 1990). A complete validation of the control and perturbed runs with this version of the model for the South American region can be found in Carril *et al.* (1997). In that paper, particular attention was given to the evaluation of the model performance regarding those variables that are important for climate impact studies and for the dynamical and thermodynamical behaviour of the model: surface air temperature, mean sea level pressure and near-surface winds.

 

Table V. Correlation coefficient, bias (°C) and root mean square error (°C) between 2 m temperature derived from the HADAM and the MPI control simulations and the NCEP re-analysis, for summer and winter months

| | HADAM | | MPI | |
|---|---|---|---|---|
| | Summer | Winter | Summer | Winter |
| COR | 0.95 | 0.96 | 0.95 | 0.93 |
| BIAS (°C) | 0.98 | 0.05 | 0.17 | 0.009 |
| RMS (°C) | 3.11 | 2.56 | 2.55 | 2.24 |

In order to test the ability of the GCM in simulating the observed climate, the present day experiments will be first evaluated specifically for our region of interest against the NCEP re-analyses data. The long-term means of the predictor variables will be analysed. Only results for temperature will be shown as it is the most relevant variable in this study. Then, the ability of the statistical method in scaling down the information given by the GCM will be examined, with the aim of evaluating whether it is possible to provide reliable estimations of the local variables. The data from the GCM outputs were first interpolated to the 2.5° grid used to fit the statistical model.

### *4.1. Control run of the HADAM and MPI GCMs*

Figure 9 shows the long-term mean 2 m temperature field for summer and winter months from the NCEP analyses and simulated with HADAM and MPI GCMs and Table V presents some measures of model performance: pattern correlation coefficient (COR), regional bias (BIAS) and root mean square error (RMS) (see Giorgi *et al.*, 1994 for definitions). The overall pattern of the temperature field is reasonably well-reproduced by both models. Nevertheless, for both summer and winter, the HADAM model is anomalously warmer than observations in the northern part of the domain, producing a greater meridional temperature gradient across the region. The differences between observed and simulated mean temperature with HADAM GCM are greater for summer months. The MPI simulated temperature field agrees quite well with the analyses, though rather colder than the analyses for winter months in the southern part of the domain.

Nevertheless, MPI model gives a climate simulation closest to the observed climate in the region of interest, and therefore, we will consider this model for the climate change large-scale estimations.

An estimation of the minimum, maximum and mean temperatures for summer and winter months are made by using the simulated large-scale predictors from the two present day simulations and the resulting local temperatures are then compared against the observations. The local temperatures estimated from GCM simulations cannot, of course, be compared directly with observations. In the comparison between observed and estimated temperatures, it should be taken into account that the observed mean is calculated for the verification period (1972–1981) and the estimated mean is obtained from a number of model years (45 years for HADAM GCM; no information was available concerning the number of model years for MPI GCM) representative of the present climate conditions.

Figures 10 and 11 show the estimated temperatures obtained from the HADAM and MPI large-scale predictors, respectively. Compared with the spatial patterns of observed temperatures in Figure 5, for summer months, it can be seen that differences between the estimated values from the HADAM model and observed minimum and mean temperatures are well within the observed interannual variability, except in the northern part of the domain, where the model mean temperature is overestimated. This results in a larger meridional temperature gradient in the estimated field compared with observations. Nevertheless, the overall pattern is reasonably well-reproduced. The differences are larger for maximum temperature, particularly in the northern part of the domain, where the estimation exceeds the observed values by more than 3°C. These differences, larger than the observed variability, are probably due to the fact that the simulated predictors do not represent the present climate adequately in that area.

 

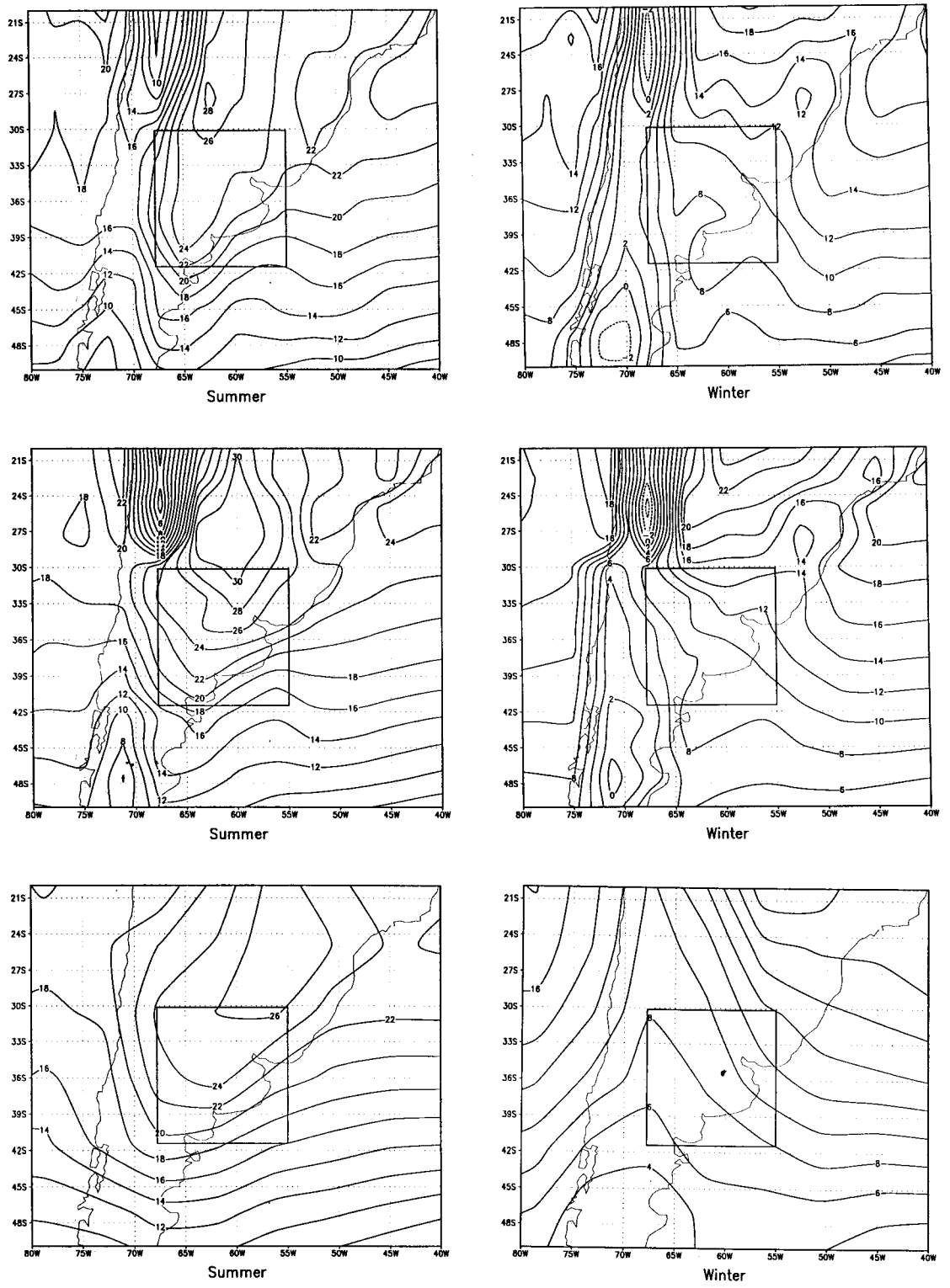


Figure 9. Mean 2 m temperature fields as derived from NCEP re-analyses (upper panels), HADAM GCM (centre panels) and MPI GCM (bottom panels) control experiments for summer months (left) and winter months (right)

 

For winter months, the differences between estimated and observed (Figures 10 and 6) minimum and maximum temperatures are larger over the entire domain. However, the estimated pattern of mean temperature shows better agreement.

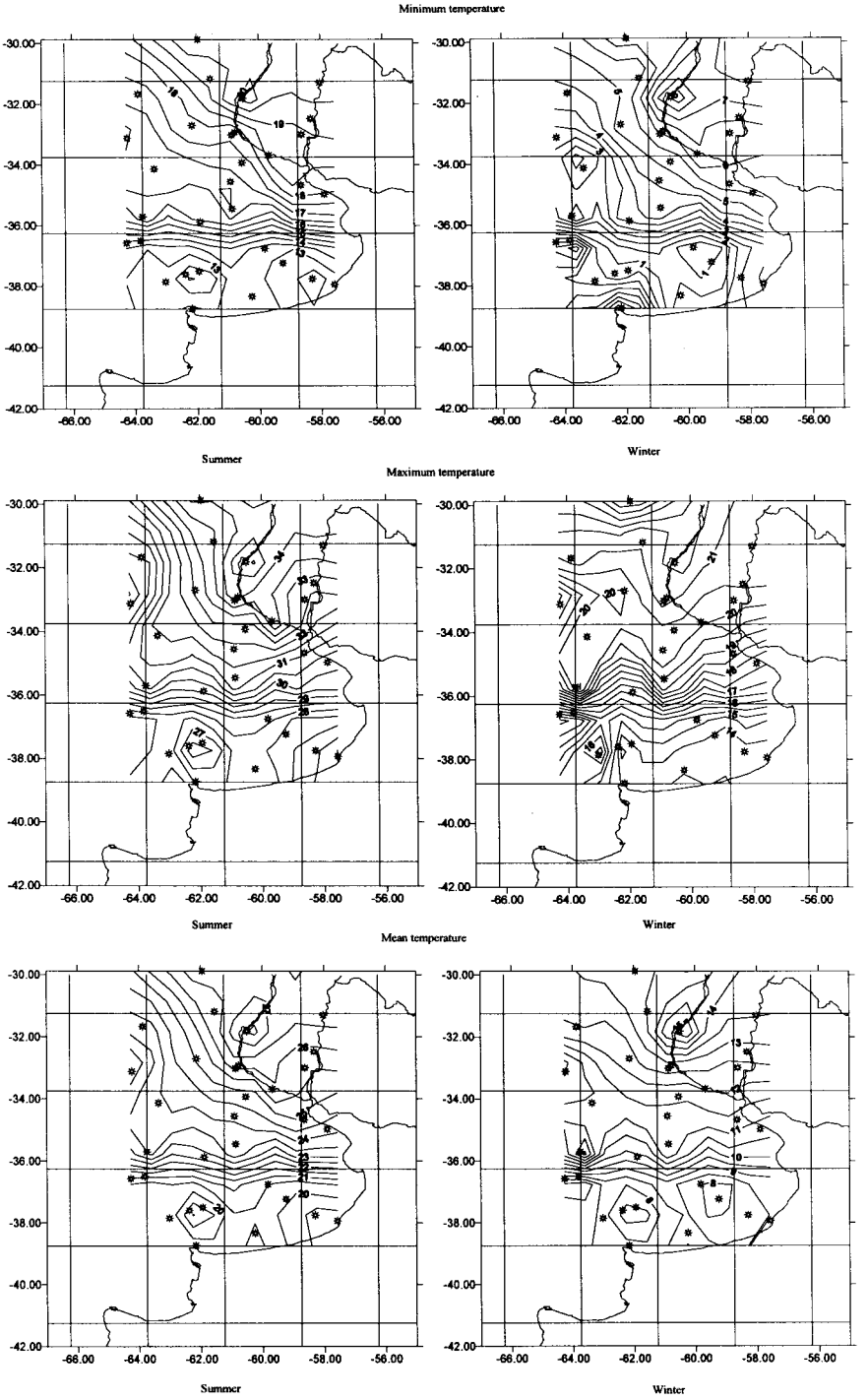


Figure 10. Estimated minimum (top), maximum (centre) and mean (bottom) temperatures from HADAM control simulation for summer months (left panels) and winter months (right panels)

 

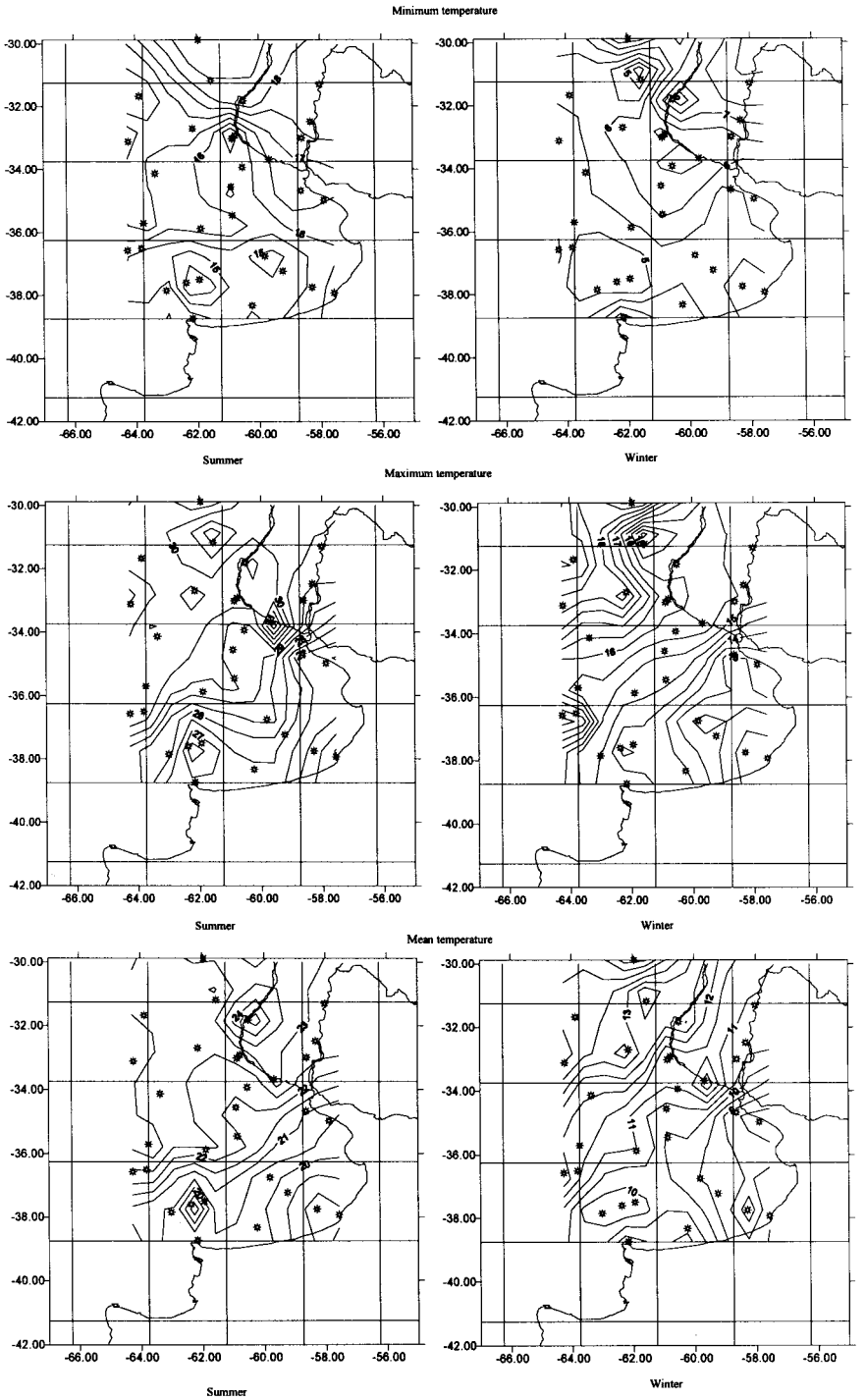


Figure 11. Same as Figure 10 for MPI control simulation

The pattern of estimated temperatures obtained using the MPI large-scale predictors (Figure 11) matches well with the observations for summer months, though minimum and mean temperatures are slightly underestimated in the southeast part of the domain. However, the summer differences are well within the range of the observed variability. For winter months, the differences between observed and

 

estimated temperatures are larger. This may be due to the fact that the MPI model is less accurate at simulating the extratropical temperatures for winter months than for summer months (Carril *et al.*, 1997). Thus, it is concluded that the dissimilarity of the estimated versus the observed mean temperatures is most likely due to the performance of the GCM simulation for winter months.

To sum up these results, we can conclude that the MPI model provides reliable estimates of the large-scale 2 m temperatures and the statistical model is able to provide information on the local scale. Hence, it is possible to project changes in the large-scale temperature forcing onto local scale monthly mean temperatures.

### *4.2. Estimation of local temperature changes*

Climate models do not simulate the present climate perfectly, as we can infer from the previous analysis. However, we can assign a degree of confidence to the simulated changes from the present to the future climate, since the GCMs do provide a good representation of the large-scale atmospheric circulation and the feedbacks involved in climate change.

The characteristics of the global scale changes simulated in the 'scenario A' experiment conducted with the MPI model for the South American region, are detailed in Carril *et al.* (1997). We will give only a brief summary of the regional features of the induced climate change. An increase of surface air temperature, maximum over the continent, is the most immediate effect in the perturbed simulation. For summer months an increase of temperature greater than 2°C over central Argentina is predicted, while for winter months the temperature increase is lower. The SLP change projected by the MPI model shows an increase in pressure over a great part of the continent, a weak intensification of the subtropical anticyclones, a deepening of the subpolar trough, and an intensification of the westerly winds. For summer months the amplitude of the pressure anomalies is lower than in winter.

Figure 12 shows the difference between the perturbed and control simulated large-scale mean temperature, which is the most relevant large-scale predictor, for summer and winter months in the region of interest. Maximum warming is located in the western part of the domain for summer months (2.4°C), and in the north-eastern part of the domain for winter months (2°C). A larger warming is projected for summer months than for winter months.

The application of the relationships derived between the local predictands and the large-scale predictors to the GCM simulated changes provides a reliable estimation of the possible anthropogenic changes in the local variables. To accomplish this, differences between the simulated predictors in the perturbed run and the control run are used as input variables to estimate possible changes in the local minimum, maximum and mean temperatures. The results are summarized in Figure 13.

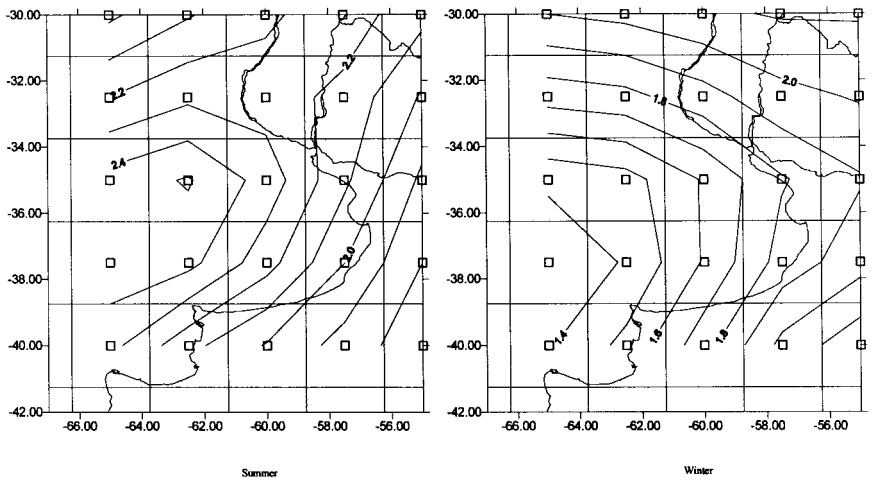


Figure 12. Temperature change ($2 \times CO_2$-CONTROL) as derived from the MPI GCM for summer months (left) and winter months (right)

 

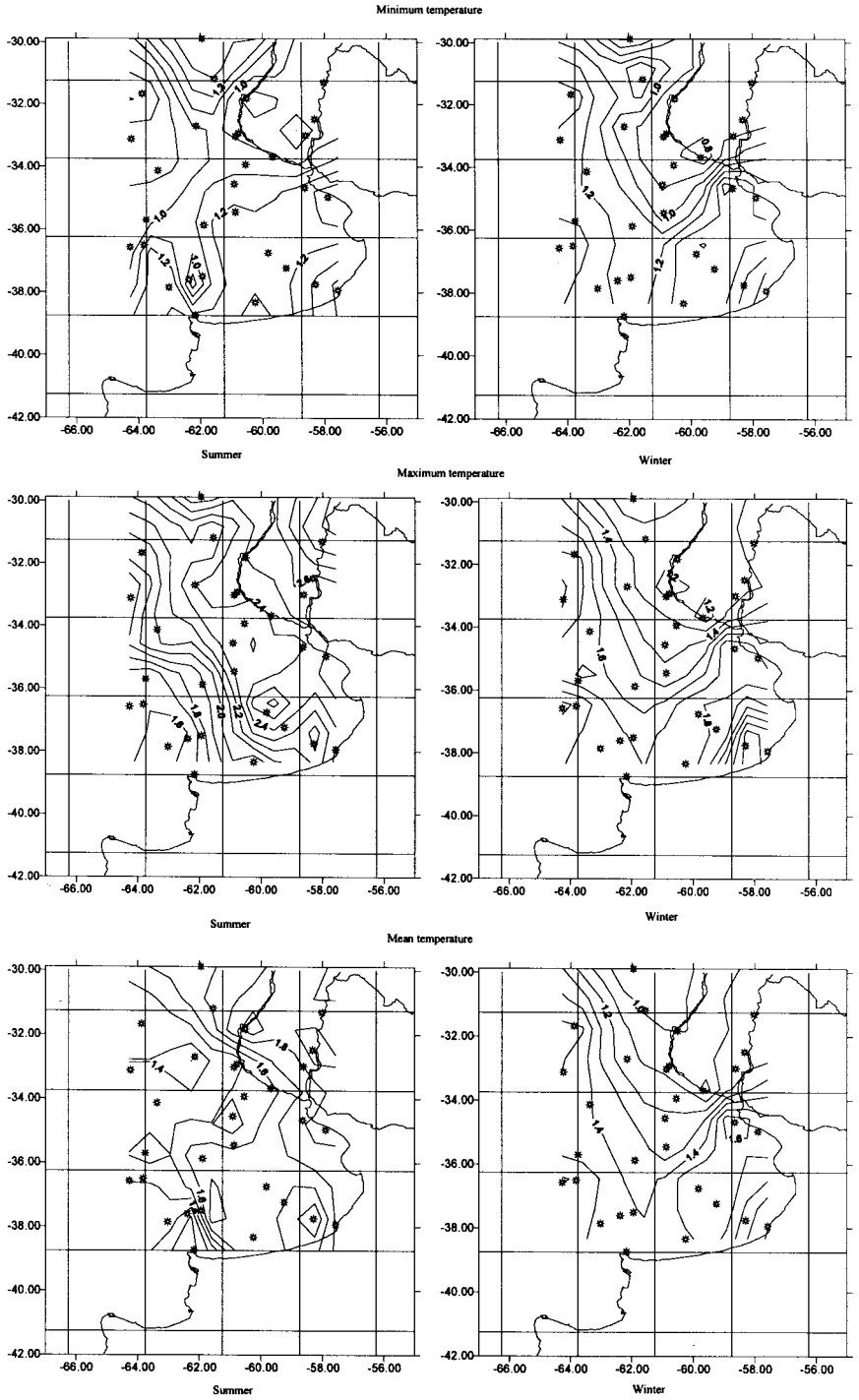


Figure 13. Minimum (top), maximum (centre) and mean (bottom) temperature change estimated from large-scale changes given by MPI GCM for summer months (left panels) and winter months (right panels)

For both summer and winter months, the temperatures increases are slightly smaller than the simulated by the GCM (as in Wilby *et al.*, 1998), and are well within the observed interannual variability range, giving a degree of confidence to the estimated anomalies. The temperature increase is smaller for

 

minimum temperature than for maximum temperature for almost all the stations, yielding an enhanced temperature amplitude in both seasons. The enhanced temperature amplitude for summer months is larger than for winter months. The estimated maximum temperature increase is found to be larger for summer months than for winter months for all the stations, while for minimum temperature, the increase for summer and winter months are similar. These conclusions may be useful for climatic change impact studies, noting that the downscaling does not provide a prediction, but rather a more reliable regional scenario. It is also worth noting that the spatial pattern of temperature increases given by the GCM is different from that estimated by the statistical model, indicating that individual site changes can differ from the grid point changes.

## 5. SUMMARY AND CONCLUSIONS

For the purposes of estimating potential temperature changes at the local scale, a statistical approach was developed to downscale grid point information produced by GCMs. Empirical relationships were derived between large-scale air temperature at 2 m, mean sea level pressure and zonal and meridional components of the wind at 200 and 700 hPa from NCEP re-analysis data (the predictors) and station minimum, mean and maximum temperatures (the predictands) for summer and winter months, making use of the interannual variations in climate, by means of a stepwise linear regression method (Wigley *et al*., 1990) for 31 stations covering the central region of Argentina. The regression equations were calibrated using data for the period 1982–1994 and tested on an independent data set, for the period 1972–1981, by estimating the predictands and comparing these with the observed values.

According to von Storch *et al*. (1993), three conditions must be fulfilled for this statistical approach to be useful: first, the statistical relationship between large-scale predictors and local scale predictands should explain a great part of the observed variability of the local variable; secondly, the large-scale parameters should be well-simulated by climate models; and thirdly, the expected changes in the mean climate should lie within the range of its natural variability, captured by the calibration data. We have checked to what extent the above assumptions are fulfilled in order to establish the degree of confidence that can be placed in the estimated changes projected at local scale.

Despite the simplicity of the statistical approach described, it was demonstrated that it is able to satisfactorily reproduce the spatial patterns and time evolution of the summer and winter months' minimum, maximum and mean station temperatures. A great part of the observed variability of the local predictands is explained by the large-scale predictors. However, the prediction skill of the statistical model varied between the stations and the seasons. In almost all cases, the estimates are less accurate during the summer months, probably due to smaller scale processes, such as convective processes, not well-captured by the large scale predictands.

The procedure was applied to the present day climate simulations provided by the HADAM and MPI GCMs, which were validated in order to check the second assumption listed above. In general, both of the GCMs are reasonably successful at simulating the major features of the observed mean predictors, although the MPI model shows better agreement when compared with the analyses. The estimated patterns of minimum, maximum and mean temperatures using the MPI simulation for the present climate compared quite well with the observations, though minimum and mean temperatures for summer months are slightly underestimated in the southeast part of the domain, partly due to the lower confidence in the GCM predictors. Nevertheless, the differences are well within the range of the observed variability. This result enables us to confirm that the technique could be used as an effective tool for downscaling large-scale information provided by the GCMs to local scales, and hence, to assess possible changes in local temperature extremes over the region of interest. However, we cannot be sure if the relationships derived between the predictors and the predictands will still be valid under future climate conditions. A fundamental assumption made by all statistical downscaling methods regards the stationarity of the relationships between large-scale predictors and local scale predictands (Wilby, 1997; Wilby *et al*., 1998). If the regression models derived are to be applicable to future climates, the model parameters must be

 

shown to be robust with respect to climate changes. In other words, the relationships between the local variables (the predictands) and the large-scale predictors must be time invariant, i.e. stationary. The successful performance of the statistical model using an independent data set, provides some confidence on the stability of the statistical relationships under climate variability experienced up to date. However, there can be no guarantee that the statistical relationships are stable to future climate scenarios. Nevertheless, since the temperature changes projected by the GCMs are well within the range of the natural variability of the observed climate (as shown by comparing Figures 2 and 12), it is possible to assume that the statistical relationships will still be valid under climate change conditions. In this context, the reliability of the application to enhanced greenhouse gases experiments should be taken as the more justifiable local estimate.

Bearing this in mind, the response of the climate system to the enhanced emission scenario simulated by the MPI model is used to infer the local temperature changes. For summer and winter months, the temperature changes are well within the observed range of interanual variability, fulfilling the third assumption cited above. For both seasons, a smaller increase was found in the minimum than in the maximum temperature, yielding an enhanced temperature amplitude. At almost all the stations, the maximum temperature increase was found to be larger for summer months than for winter months, while minimum temperature increases were similar for both seasons.

It should be pointed out that the reliability of the results presented in this study, regarding the future changes in local temperature, are highly dependent on the reliability of the GCM simulated large-scale changes. Though all general circulation models project a global scale temperature increase, there are differences in the spatial patterns and the magnitude of the warming (Henderson-Sellers and Hansel, 1995). With the improvement of current climate models, in terms of resolution, parameterizations and atmosphere–ocean interactions, our uncertainty in this respect will be greatly reduced.

The statistical method described is based on grid point information, and current GCMs have little predictive capability at the individual grid points. Nevertheless, the information deduced at the local scale from control experiments shows considerable agreement when compared with observed values.

Despite the encouraging results shown, the method has some limitations. One of the uncertainties, as in all statistical approaches, is the non-stationartiy of the time series used in the analysis. We should also point out that longer time series should yield more consistent results, as a greater range of natural variability would be considered. Improved results might be obtained by using more sophisticated techniques, such as the method described by von Storch *et al*. (1993), in which a larger spatial domain for the predictor variables is used to specify the local parameters, since the GCMs performs better at such scales.

## ACKNOWLEDGEMENTS

This work has been supported by the European Commission under contract CEE C11-CT94-0111. The authors wish to thank Dr Peter Rowntree for providing HADAM GCM data. The NCEP re-analyses data were obtained through ftp, with the help of Wesley Ebisuzaki. The station data were provided by people from INTA. The authors also wish to thank Dr Walter Vargas for useful and helpful comments on several aspects of this study. The constructive comments of two anonymous referees were also much appreciated.

## REFERENCES

Bardossy, A. and Plate, E. 1992. 'Space-time model for daily rainfall using atmospheric circulation patterns', *Water Resour. Res.*, **28**, 1247–1259.

Burger, G. 1996. 'Expanded downscaling for generating local weather scenarios', *Clim. Res.*, **7**, 111–128.

Burkhardt, U. 1995. 'Validation of the small-scale performance of a climate model', *Clim. Dyn.*, **11**, 299–305.

Carril, A., Menéndez, C. and Nuñez, M. 1997. 'Climate changes scenarios over South American region: an intercomparison of coupled general atmosphere–ocean models', *Int. J. Climatol.*, **17**, 1613–1633.

Conway, D., Wilby, R.L. and Jones, P.D. 1996. 'Precipitation and air-flow indices over the British Isles', *Clim. Res.*, **7**, 169–183.

 

Corte-Real, J., Zhang, X. and Wang, X. 1993. 'Downscaling GCM information to regional scales: a non-parametric multivariate regression approach', *Clim. Dyn.*, **11**, 413–424.
Cubasch, U., Hasselmann, K., Hock, H., Maier-Reimer, E., Mikolajewicz, U., Santer, B. and Saunsen, R. 1992. 'Time-dependent greenhouse warming computations with a coupled ocean–atmosphere model', *Clim. Dyn.*, **8**, 55–69.
Cullen, M.J.P. 1993. 'The unified forecast/climate model', *Meteorol. Mag.*, **122**, 81–94.
Déqué, M. and Piedelievre, J. 1995. 'High resolution climate simulation over Europe', *Clim. Dyn.*, **11**, 321–339.
Enke, W. and Spekat, A. 1997. 'Downscaling climate models outputs into local and regional weather elements by classification and regression', *Clim. Res.*, **8**, 195–207.
Giorgi, F. 1990. 'Simulation of regional climate using a limited area model nested in a general circulation model', *J. Clim.*, **3**, 941–963.
Giorgi, F, Brodeur, C.S. and Bates G. 1994. 'Regional climate change scenarios over United States produced with a nested regional climate model', *J. Clim.*, **7**, 375–399.
Grotch, S. and MacCracken, M.C. 1991. 'The use of general circulation models to predict regional climate change', *J. Clim.*, **4**, 286–303.
Henderson-Sellers, A. and Hansel, A.M. 1995. *Climate Change Atlas: Greenhouse Simulations from the Model Evaluation Consortium for Climate Assessment*, Rosen, R. (ed.), Kluwer Academic, London, p. 160.
Hewitson, B. 1994. 'Regional climates in the general circulation model: surface air temperature', *J. Clim.*, **7**, 283–303.
Hughes, J.P., Lettenmaier, D.P. and Guttorp, P. 1993. 'A stochastic approach for assessing the effect of changes in regional circulation patterns on local precipitation', *Water Resour. Res.*, **29**, 3303–3315.
IPCC, 1990. *Climate Change. The IPCC Scientific Assessment*, WMO/UNEP, Houghton, J.T., Jenkins, G.J. and Ephramus, J.J. (eds.), Cambridge University Press, Cambridge, p. 365.
Jones, R.G., Murphy, J.M., Noguer, M. and Keen, B. 1997. 'Simulation of climate change over Europe using a nested regional-climate model. II: Comparison of driving and regional model responses to a doubling of carbon dioxide', *Q. J. R. Meteorol. Soc.*, **123**, 265–292.
Kalnay, E., Kanamitsu, M., Kistler, R., Collins, W., Deaven, D., Gandin, L., Iredell, M., Saha, S., White, G., Woollen, J., Zhu, Y., Chelliah, M., Ebisuzaki, W., Hoggins, W., Janowiak, J., Mo, K.C., Ropolewski, C., Wang, J., Leetmaa, A., Reynolds, R., Jenne, R. and Joseph, D. 1996. 'The NCEP/NCAR 40-year reanalysis project', *Bull. Am. Meteorol. Soc.*, **77**, 437–471.
Karl, T.R., Wang, W.C., Schlesinger, M.E., Knight, R.W. and Portman, D. 1990. 'A method of relating general circulation model simulated climate to observed local climate. Part I: Seasonal statistics', *J. Clim.*, **3**, 1053–1079.
Katz, R.W. and Parlange, M.B. 1996. 'Mixtures of stochastic processes: application to statistical downscaling', *Clim. Res.*, **7**, 185–193.
Kilsby, C.G., Cowpertwait, P.S., O'Connell, P.E. and Jones, P.D. 1998. 'Predicting rainfall statistics in England and Wales using atmospheric circulation variables', *Int. J. Climatol.*, **18**, 523–539.
Labraga, J.C. 1997. 'The climate change in South America due to a doubling in the $CO_2$ concentration: intercomparison of general circulation model equilibrium experiments', *Int. J Climatol.*, **17**, 377–398.
Leslie, L.M. 1995. 'A new general circulation model: formulation and preliminary results in a single and multi-processor environment', in *Abstracts New South Wales Climate Symposium*, Sydney, Australia, September 20–21.
McGinnins, D.L. 1994. 'Predicting snowfall from synoptic circulation: a comparison of linear regression and neural network', in Hewitson, B.C. and Crane, R.G. (eds.), *Neural Nets: Applications in Geography*, Kluwer Academic, Boston, pp. 79–99.
Murphy, J.M. 1995. 'Transient response of the Hadley Centre coupled ocean–atmosphere model to increasing carbon dioxide. Part I. Control climate and flux correction', *J. Clim.*, **8**, 496–514.
Noguer, M. 1994. 'Using statistical techniques to deduce local climate distributions. An application for model validation', *Meteorol. Appl.*, **1**, 277–287.
Schubert, S. and Henderson-Sellers, A. 1997. 'A statistical model to downscale local daily temperature extremes from synoptic-scale atmospheric circulation patterns in the Australian region', *Clim. Dyn.*, **13**, 223–234.
von Storch, H., Zorita, E. and Cubasch, U. 1993. 'Downscaling of climate change estimate to regional scales: application to winter rainfall on the Iberian Peninsula', *J. Clim.*, **6**, 1161–1171.
von Storch, H. 1994. *Inconsistencies at the Interface of Climate Impact Studies and Global Climate Research*, Technical Report 122, Max Plank Institut fuer Meteorologie, Hamburg, Germany, p. 25.
Wigley, T.M., Jones, P., Briffa, K. and Smith, G. 1990. 'Obtaining subgrid scale information from coarse resolution general circulation output', *J. Geophys. Res.*, **95**, 1943–1953.
Wilby, R.L. 1997. 'Non-stationarity in daily precipitation series: implications for GCM downscaling using atmospheric circulation indices', *Int. J Climatol.*, **17**, 439–454.I
Wilby, R.L., Hassan, H. and Hanaki, K. 1998. 'Statistical downscaling of hydrometeorological variables using general circulation model output', *J. Hydrol.*, **205**, 1–19.
Wilks, D.S. 1992. 'Adapting stochastic weather generation algorithms for climate change studies', *Clim. Change*, **22**, 67–84.
Winkler, J.A., Palutikof, J.P., Andresen, J.A. and Goodess, C.M. 1997. 'The simulation of daily temperature time series from GCM output. Part II: sensitivity analysis of an empirical transfer function methodology', *J. Clim.*, **10**, 2514–2532.
Zorita, E., Hughes, J.P., Lettemaier, D.P. and von Storch, H. 1995. 'Stochastic characterization of regional circulation patterns for climate model diagnosis and estimation of local precipitation', *J. Clim.*, **8**, 1023–1042.

 